ISSN: 0974-2115
www.jchps.com Journal of Chemical and Pharmaceutical Sciences

Study of lower D-region of ionosphere from VLF signal perturbations

Rashmi G*, Shanmuga Sundaram G A
Center for Excellence in Computational Engineering and Networking, Amrita Vishwa Vidyapeetham, Coimbatore, India.
***Corresponding author: E-Mail: rashmisatya64@gmail.com**

ABSTRACT

VLF signal analysis is an effective remote sensing tool to study the conditions and disturbances in ionosphere and hence the level of activity in the sun. The observation of solar flares made during the months of April to June 2015 is presented. The electron density of the ionosphere during the flare onset is also assessed using the International Reference Ionosphere model (IRI). The VLF signals are recorded at receiver site located at Ettimadai, Coimbatore (10.8981ºN, 76.9003ºE) from the transmitting station VTX (17 kHz) located at South Vijayanagaram, Tuticorin (8.387014ºN, 77.752761ºE) with Great Circle Path of 294km. The GOES satellite x-ray flux data is used for determining the onset and duration of flare and thus the time delay at the receiver site is assessed.

KEY WORDS: Electron density, GOES satellite, IRI, Solar flares, VLF signals, VTX.

1. INTRODUCTION

The field of space weather monitoring is gaining importance in the recent years. The sun's activity manifested in the form of solar flares or Coronal Mass Ejection (CME) has a direct impact on the ionosphere. It is essential to monitor the conditions in the sun because it has direct impact on our life owing to our ever increasing dependency on sophisticated technologies and communication systems. Solar flares produce strong x-rays that block high-frequency radio waves that we use for radio communication and this phenomenon is termed as Radio Blackout Storms in addition to this energetic proton from sun can penetrate satellite electronics and cause electrical failure.

In addition to this, CMEs can lead to geomagnetic storms at earth resulting in the induction of extra currents in the ground that can impact the power grid operations. The emission of hard and soft x-ray radiation because of solar flares influence the earth's atmosphere and additionally the propagation of Very Low Frequency (3 - 30 kHz) waves via Earth Ionosphere Wave Guide (EIWG), found approximately 60 to 70 km over the earth surface. The particles in the upper atmosphere get ionized by the radiation and the ionosphere is created which is defined as a conducting layer that is located at an altitude of around 50 and 1500 km. The ionosphere is partitioned into three different layers namely F, E and D layers. The F layer can be split into the F1 and F2 layers. Since the primary factor of ionization of these layers, is solar radiation, the electron density in these layers changes from day to night. During day time condition, the ionospheric propagation occurs at a height of 70 km. The Lyman-α radiation (121 nm) from the sun increases electrical conductivity at this altitude by ionizing Nitric Oxide (NO) resulting in this propagation. However, at night time, the electron recombination processes takes a lead over the ionization resulting in the D-region disappearance and the reflecting layer thus increases to an altitude of 90 km.

The electron density of ionosphere normally increases from the height of 50 km. Ionospheric layer that is fundamental from our paper's perspective of flare identification is alluded to as the 'D-layer' (at 50 km to 90 km height) and the 'lower E-layer' (90 km to 150 km height). At VLF and LF, given at frequencies below 300 kHz, the D-layer serves as reflecting layer by which these frequencies could propagate worldwide. The ionosphere exhibits a diurnal (day/night), a seasonal (summer/winter) and strong relationship with increased activity of the sun. Several works have been done before to illustrate the relationship between the level of activity in the sun and the subsequent changes in the ionosphere from VLF signal analysis. Studied the amplitude perturbations at D-region during solar minimum, used Long Wave Capability Code (LWPC) to calculate the variations in height and the sharpness of the ionosphere during varying intensities of the solar flares and also electron densities with the same. Additional analysis of correlation between amplitude and phase perturbations with flux is done. In our paper about 10 B-flares, 24 C-flares, 10 M-flares were observed and the electron density is also estimated using the IRI model and the results are tabulated.

Solar flares: Solar flares are huge blasts happening on the surface of the sun which discharge a vast measure of particles. Protons are likewise emitted during bigger flares. During solar flares the emitted radiation and plasma are warmed to millions of degrees Celsius leaving the sun in an enormous arc. In the time spanning a few minutes, a solar flare can release large amount of energies in the range of 10^{22} to 10^{25} Joules. These flares occur from sunspots. Solar flares are named A, B, C, M or X on the basis of the peak flux (in watts per square meter, W/m^2) as measured on the GOES satellite. Every class will have a peak flux ten times more than the previous one. For example, X class flares the most powerful of all flares, has a peak flux of 10^{-4} W/m^2. Within a class itself, a linear scale from 1 to 9 is utilized, in this way an X2 flare is twice as capable as an X1 flare, and is five times more effective than a M4 flare. Among the flares the X-class flares have the largest impact when it is directed towards earth and can cause long periods of radio blackouts. These happen on the dayside of earth and are intense when the sun is specifically overhead. M-class flares are slightly medium flares and then can cause a short term radio blackout. The C-class and B-class flares cause less disturbances on a comparative basis.

2. MATERIALS AND METHODS

The loop antenna is used to capture VLF signals in the range of (3-30 kHz) and is connected to the microphone input of the computer. A PC 16 bit with a 44100 Hz sound card microphone input is capable of detecting small discrepancies in voltage at frequencies less than 20 kHz and acts as the VLF receiver. For the purpose of analyzing the signals software called 'Spectrum Lab' is used.

This set up aids in continuous monitoring of amplitude and phase variations of various VLF signals that are transmitted from VLF stations from various locations of the world. VTX (17 kHz) transmitter located at and NWC (19 kHz), Australia located at are clearly tunable at our receiver site located at Ettimadai, TamilNadu.

The audio signals recorded by the sound card require an effective spectrum analyzer for further research purposes. The spectrum lab is effective software for analysis of audio signals spectrum change and plotting the data. Sophisticated post processing of the recorded data is available where we can export our continuously recording readings in a text file format. In our work, once the text files with the amplitude data are available for various stations we use matlab program for visualizing and denoising.

Figure.1.The VLF loop antenna and system running the spectrum lab software

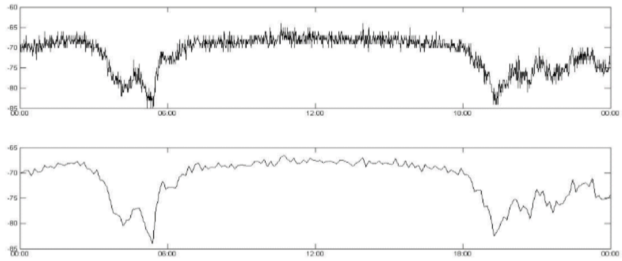

Fig 2.The recorded signal and denoising using soft wavelet thresholding

Denoising the recorded VLF signal: VLF signals are very noisy due to environmental conditions and no analysis can be carried on without denoising as there is a risk of missing out small variations in the signals that indicate a B-class or C-class flare. For this purpose we use wavelet based denoising that implements soft thresholding using the idea given
. Accordingly the soft wavelet thresholding is given as,

$$y = \begin{cases} sign(x).(|x| - \Delta x) & if\ |x| > \Delta x \\ 0 & otherwise \end{cases}$$

The variations in recorded and denoised signal are clearly visible from Fig 2.

IRI Model: Committee on Space Research (COSPAR) and the International Union of Radio Science (URSI) devised an empirical standard model for the ionosphere that takes given latitude, longitude, time hours and date as input and provides the electron density, temperature of ions and electrons at the ionospheric layer, and ion composition in the altitude range of 50 km to about 2000 km on the given day. Using this model we can assess the condition of ionosphere as well as solar zenith angle during each event of the flare.

3. RESULTS AND DISCUSSIONS

The signal analysis is done for the April to June 2015 data and the following observations are made.

B class flare: On May 19 a B9 class flare was observed from 7:28 (UT) till 8:00 (UT) and the delay observed in the recorded VLF perturbations is shown in the Fig 3. The rise time and fall time of the flare is found to be 8 min and 7 min respectively. We find that the B-flare starts at 7:40 (UT) in our recordings, reaches the peak time at 7:49 (UT) showing a 11 minutes time delay from GOES satellite data.

M class flare: On April 21 a M4 class flare was observed from 15:25 (UT) till 16:25 (UT) and the delay observed in the recorded VLF perturbations is shown in the Fig 4. The rise time and fall time of the flare is found to be 9 min and 8 min respectively. A time delay of 3 min is observed. In our recorded VLF signal the flare begins at 15:43 (UT) and reaches peak at 15:51 (UT).

C class flare: On June 5 a C1 class flare was observed from 7:00 (UT) till 7:18 (UT) and the delay observed in the recorded VLF perturbations is shown in the Fig 5. The rise time and fall time of the flare is found to be 2 min and 9 min respectively as a downward peak is observed and in our recorded data shows the C-flare beginning from 7:11 (UT) and peak time to be 7:20 (UT). A time delay of 11min is observed for the starting time and peak is reached at a delay of 2 min.

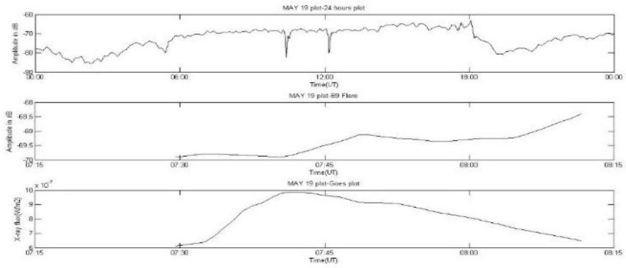

Fig.3.Observed B-class flares at receiver site and GOES data

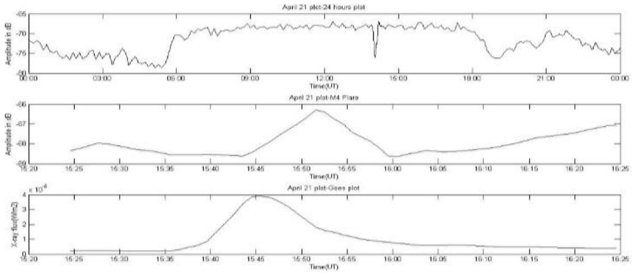

Fig.4.Observed M-class flares at receiver site and GOES data

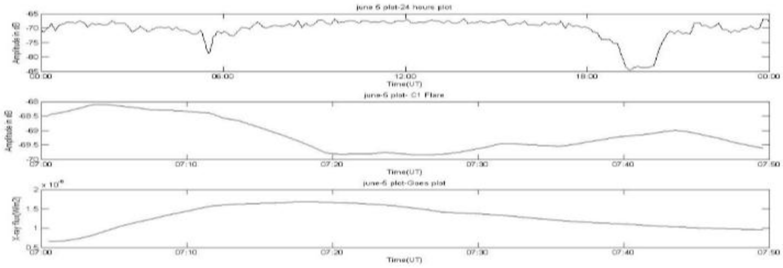

Fig.5.Observed C-class flares at receiver site and GOES data

Table.1 Electron density and solar zenith angle calculation from IRI model

Day	Flare type	Electron density (Ne) at (74km)	Solar zenith Angle in Degrees	Flare start time (UT)
May 19	B9	0.51283E+09	13.1	7:28
May 22	B4	-0.10000E+01	120.5	15:24
May 23	C1	0.40382E+09	49.4	3:27
April 21	C4	0.24799E+09	69.7	2:00
April 21	C3	0.22342E+09	76.3	1:38
April 22	M1	0.50522E+09	24.3	8:30
June 13	M1.3	0.50763E+09	13.9	7:20
June 14	M2	0.20300E+09	82.1	1:08

4. CONCLUSION

This paper analyses the ionospheric response to solar activity for the duration of three months. From the plots obtained the time delay associated with each flare is evident. Usually the delay observed is approximately 7-8 minutes from the GOES satellite data. Also from the table we observe that with higher class of flare observed an increased electron density is observed. It is also to be noted that solar zenith angle also plays a significant role in determining the electron density. The work can be made more effective by finding a model for the ionospheric disturbances by finding signature pattern of each flare that will lead to a better understanding of impact on the ionosphere.

REFERENCES

Abhikesh Kumar, and Sushil Kumar, Space weather effects on the low latitude D-region ionosphere during solar minimum, Earth, planets and space, 2014, 66-76.

Alan Melia, Flare Detection using VLF Radio signals, Radio Society of Great Britain (RSGB) Propagation Studies Committee, 2010.

Esat Guzel, Murat Canyılmaz, and Mustafa Turk, Application of wavelet-based denoising techniques to remote sensing very low frequency signals, Radio Science, 46, 2011.

Grubor D.P, Sulic D.M, and Zigman V, Classification of X-ray solar flares regarding their effects on the lower ionosphere electron density profile, Annales Geophysicae, 26, 2008, 1731–1740.

Mohd Masri Abd Rashid, Mahamod Ismail, Alina Marie Hasbie, Mohammad Mohammadpour Salut, and Mardina Abdullah, VLF Observation of D-Region Disturbances Associated with Solar Flares at UKM Selangor Malaysia, Proceeding of the 2013 IEEE International Conference on Space Science and Communication (Icon Space), 2013.

Nicolet M, and Aikin A.C, The Formation of the D Region of the Ionosphere, Journal of Geophysical Research, 65, 1960, 1469-1483.

Thomson N.R, D-Region Electron Distributions in Middle Latitudes Deduced from the Reflection of Long Radio Waves, Proceedings of the Royal Society of London, Series A, Mathematical and Physical Sciences, 291, 1993, 413-437.